Articles

Use of Lanthanide-Induced Nuclear Magnetic Resonance Shifts for Determination of Protein Structure in Solution: EF Calcium Binding Site of Carp Parvalbumin†

Lana Lee‡ and Brian D. Sykes*

ABSTRACT: The binding of the paramagnetic lanthanide ion ytterbium to the calcium binding protein carp parvalbumin results in a series of ^{1}H NMR resonances which are shifted far outside the envelope of the ^{1}H NMR spectrum of the diamagnetic form of the protein; bound Yb^{3+} also induces shifts in the ^{13}C NMR spectrum of parvalbumin and in the ^{113}Cd NMR spectrum of cadmium-substituted parvalbumin. The interpretation of these lanthanide-shifted resonances in terms of the structure of the protein surrounding the metal binding site requires the determination of the orientation and principal elements of the magnetic susceptibility tensor of the protein-bound Yb^{3+} ion. A previous comparison [Lee, L., & Sykes, B. D. (1982) *Biomolecular Structure Determination by NMR* (Bothner-By, A. A., Glickson, J. D., & Sykes, B. D., Eds.) pp 169–188, Marcel Dekker, New York] of the observed Yb^{3+}-shifted ^{1}H NMR spectrum of parvalbumin with a calculated spectrum, based upon the X-ray structure and an initial determination of the magnetic susceptibility tensor, led to the conclusion that there were significant differences between the solution and X-ray structures. In this paper, the magnetic susceptibility tensor has been reevaluated with the aid of newly assigned ^{13}C and ^{113}Cd NMR resonances. The agreement between the calculated and observed spectra is now close overall.

The elucidation of the X-ray crystallographic structure of the calcium binding protein parvalbumin from carp reveals that each of its two calcium binding sites is contained in a contiguous polypeptide sequence which forms in turn a helix, a loop around the metal ion, and a second helix. The loop around the metal ion contains regularly spaced carboxyl, carbonyl, and hydroxyl ligands. These calcium binding domains have been labeled the "CD and EF hands" (Kretsinger & Nockolds, 1973). Homologous sequences to the CD and EF calcium binding domains of parvalbumin can be found in rabbit skeletal troponin C (Collins et al., 1977), the myosin light chains (Collins, 1974; Weeds & McLachlan, 1974), the 5,5′-dithiobis(2-nitrobenzoic acid) (DTNB) light chains (Collins, 1976), bovine calmodulin (Vanaman et al., 1977; Stevens et al., 1976), rat testis calmodulin (Dedman et al., 1978), bovine intestinal calcium binding protein (Fullmer & Wasserman, 1977), porcine intestinal calcium binding protein (Hofmann et al., 1979), and other calcium binding proteins (Kretsinger, 1976). The number of times in a given protein the sequence repeats and the substitutions in the sequence can be correlated with the number of metals bound to the protein and their binding strengths, respectively (Weeds et al., 1977). These findings have led to the proposal that homologous structures, at least at the level of the calcium binding sites, exist for all these proteins.

In separate papers (Lee & Sykes, 1980a,b, 1982), we have discussed the development of an NMR methodology, the final goal of which is to compare the structures of calcium binding proteins in solution. This technique will enable us to test the hypothesis that all of these calcium binding proteins have homologous structures. The technique is based upon the substitution of paramagnetic lanthanide ions for the calcium ions bound to the protein and the subsequent analysis of the shifts and broadenings induced in the NMR spectrum in terms of the structure of the protein. We have presented the analysis of the lanthanide-induced line broadening in terms of the distance between the lanthanide metal ion and the nucleus corresponding to the lanthanide-shifted resonance (Lee & Sykes, 1980c). We have also used the lanthanide-shifted resonances to determine the relative affinities of the two calcium binding sites of parvalbumin for Yb^{3+} with respect to calcium and to observe the sequential filling of the two sites by Yb^{3+} (Lee & Sykes, 1981).

It is the lanthanide-induced shifts, however, which are the most sensitive monitors of the precise geometrical orientation of each nucleus relative to the metal ion. Unfortunately, the values of several parameters in the general equation relating the lanthanide-induced shifts to the three-dimensional structure are unknown a priori; these parameters are the orientation and principal elements of the magnetic susceptibility tensor for Yb^{3+} bound to the protein. An initial determination of the orientation and principal elements of the magnetic susceptibility tensor for Yb^{3+} bound in the EF site of carp parvalbumin (p*I* 4.25) has been reported (Lee & Sykes, 1982). The analysis was based upon three assigned resonances (the His-26 C2 and C4 protons and the amino-terminal acetyl protons) and six resonances identified as methyl resonances. Subsequent comparison of the ^{1}H NMR spectrum of the nuclei surrounding the EF metal binding site with the spectrum calculated by using the X-ray crystallographic structure led to the conclusion that the solution structure as determined by the NMR technique differed significantly.

In this paper, we present a reevaluation of the principal axis system of the magnetic susceptibility tensor for Yb^{3+} bound to the EF site of carp parvalbumin. We include in our analysis a newly assigned resonance, the ^{113}Cd NMR resonance of Cd^{2+} bound to the CD site of parvalbumin, and a ^{13}C NMR reso-

† From the Medical Research Council Group on Protein Structure and Function and the Department of Biochemistry, The University of Alberta, Edmonton, Alberta, Canada T6G 2H7. *Received March 30, 1983.* This work was supported by the Medical Research Council of Canada Group on Protein Structure and Function and by a NATO travel grant.

‡ Present address: Department of Biochemistry, Wayne State University, Detroit, MI 48201.

0006-2960/83/0422-4366$01.50/0

nance, the ζ-carbon of Arg-75. The overall agreement between the observed spectrum and the spectrum based upon the X-ray crystallographic structure is found to be very much improved.

Theory of the Lanthanide-Induced Shifts

When a paramagnetic lanthanide ion (excluding the isotropic Gd^{3+}) is substituted for one or both of the calcium ions of parvalbumin, shifted resonances appear in the NMR spectrum distinct from the corresponding spectrum of the calcium-containing protein [see Lee & Sykes (1980a–c, 1981, 1982)]. The shifted peaks are in the NMR slow exchange limit because the inverse of the lifetime of the Yb^{3+}–parvalbumin complex is smaller than any of the lanthanide-induced shifts for the observed resonances (Lee & Sykes, 1980a,b; Corson et al., 1983). The shifted resonances, which represent the spectrum of the protein–paramagnetic metal ion complex, result from the influence of the 4f electrons of the lanthanide metal on nearby nuclei and can be divided into two contributions. The first is a through-space dipolar ("pseudocontact") interaction. The magnitude of the pseudocontact shift is a function of the metal ion involved and of the geometry of the nucleus relative to the metal ion. The shift of the nucleus from its diamagnetic position, written in the principal axis system of the magnetic susceptibility tensor of the metal ion (Bleaney, 1972), is

$$\delta_P = A1\left\langle \frac{3\cos^2\theta - 1}{r^3} \right\rangle + A2\left\langle \frac{\sin^2\theta \cos 2\phi}{r^3} \right\rangle \equiv A1 \cdot G1 + A2 \cdot G2 \quad (1)$$

where $A1$ and $A2$ are parameters related to the principal elements of the magnetic susceptibility tensor of the metal ion, θ, ϕ, and r are the spherical coordinates of the nucleus in the principal axis system, and the broken brackets indicate that the appropriate time-averaged geometry of the nucleus must be used in the calculation (Briggs et al., 1972).

The second contribution to the shifts is a through-bond contact interaction which we assume is negligible. This contribution is important for directly bonded nuclei whereas we are looking at nuclei at least several bonds removed. We further minimize this contribution by the choice of metal, since the geometric dependence of this contribution is not known a priori. We have chosen Yb^{3+} because the ratio of the pseudocontact shift to the contact shift is the largest, and the absolute value of the contact shift is the smallest, for Yb^{3+} when compared to the other lanthanides (Reuben, 1973). Other criteria relevant to the expected resolution in the lanthanide-shifted spectrum are discussed elsewhere (Lee & Sykes, 1980a).

We must therefore determine the orientation in the protein of the principal axis system of the magnetic susceptibility tensor of Yb^{3+} and the two parameters $A1$ ($=X_{zz} - \bar{X}$) and $A2$ ($=X_{xx} - X_{yy}$) where X_{xx}, X_{yy}, and X_{zz} and $\bar{X}$ are the principal elements and trace, respectively, of the magnetic susceptibility tensor. We assume that the Yb^{3+} is located at the same position as the Ca^{2+} and that the coordinates of the proton nuclei can be calculated from the coordinates of atoms observed by X-ray crystallographic methods by using standard C–H and N–H bond lengths and C–C–H and C–N–H bond angles. There are five unknowns (Marinetti et al., 1977): three to describe the orientation of the principal axis system and the two scaling parameters $A1$ and $A2$. We describe the orientation of the principal axis system in terms of the direction cosines $L1$, $L2$, and $L3$ of a rotation axis (where $L1^2 + L2^2 + L3^2 = 1$) and the rotation angle α for the transformation of the coordinates of the nuclei from the X-ray structure axis system to the new principal axis system. This set of three unknowns is represented as $L1$, $L2$, and α.

Experimental Procedures

NMR Procedure. ^1H NMR spectra were obtained on a Bruker HXS-270 spectrometer operating in the Fourier-transform mode with quadrature detection. Typical instrumental settings for these spectra were 0.8-s acquisition time, +/−2.5-kHz sweep width, 8192 data points, and 1-Hz line broadening. Residual HDO was saturated by using pulsed homonuclear decoupling. The sample temperature was 303 K. The standard filters on the HXS-270 spectrometer were replaced with Bessel filters (Ithaco Model 4302).

The ^{113}Cd NMR spectra were obtained in the laboratory of Professor Sture Forsén at 56.5 MHz on a homemade NMR spectrometer employing a wide-bore superconducting magnet operating at 6.0 T. The following parameters were used to obtain the spectra: 20000-Hz spectral width, 0.56 s between pulses, 10-Hz line broadening, 45° (6-μs pulse width) flip angle, and 30000 or 100000 transients. A $Cd(ClO_4)_2$ solution was used as an external reference (where positive shifts are downfield shifts).

The ^{13}C NMR spectra were obtained at 100.6 MHz on a Bruker WH-400 NMR spectrometer. The following parameters were used to obtain the spectra: 25000-Hz spectral width, 0.66-s acquisition time, 3.66-s delay between pulses, 3-Hz line broadening, 90° flip angle (21 μs), and 17000 transients.

Sample Preparation. Stock ytterbium solutions were prepared from dried Johnson-Matthey ultrapure oxides as discussed earlier (Birnbaum & Sykes, 1978). The Yb^{3+} concentrations were determined by ethylenediaminetetraacetic acid (EDTA) titrations in pH 6 2-(*N*-morpholino)ethanesulfonic acid (Mes) buffer by using xylenol orange as an indicator.

Carp parvalbumin (p*I* 4.25) was isolated by the method of Pechere (Pechere et al., 1971). The purity and identity of this isotype were confirmed by gel electrophoresis studies, ultraviolet absorption spectra, and amino acid analysis.

The NMR samples for ^1H NMR were prepared by dissolving the lyophilized protein in the standard D_2O buffer consisting of 15 mM piperazine-*N*,*N*-bis(2-ethanesulfonic acid) (Pipes), 0.15 M KCl, 10 mM dithiothreitol (DTT), and 0.5 mM sodium 4,4-dimethyl-4-silapentane-1-sulfonate (DSS), pH 6.6. Samples for ^{13}C NMR were prepared in 0.15 M KCl–5 mM Pipes, pH 6.5. pH measurements were made with an Ingold microelectrode (Model 6030-04) attached to a Radiometer 26 pH meter. The pH values quoted are those observed and are not corrected for the deuterium isotope effect. Protein concentrations were determined by amino acid analysis after 24 h of acid hydrolysis at 110 °C. Microliter aliquots of a Yb^{3+} solution prepared at pH 6.6 were added directly to the protein solution in the NMR tube. Such additions did not affect the pH of the resulting protein solution.

Samples from ^{113}Cd NMR were prepared by adding 2 equiv of $^{113}Cd^{2+}$ to the parvalbumin and then dialyzing against 50 mM cacodylate buffer, pH 6.4. This procedure was repeated twice.

Results

We have previously reported the ^1H NMR chemical shifts for the C2 and C4 protons of His-26, and for the methyl resonance of the acetylated amino terminus, of carp parvalbumin (p*I* 4.25) in the presence of calcium and with Yb^{3+} in the EF calcium binding site (Lee & Sykes, 1982). The difference between these shifts provides the paramagnetic con-

Table I: Chemical Shift Data for the Assigned Resonances of Parvalbumin

nucleus	δ_P[a] obsd	δ_P[a] calcd	r (Å)[b]
^{1}H His-26 C2H	0.485	0.475	13.6
^{1}H His-26 C4H	0.343	0.332	15.1
^{1}H *N*-acetyl CH_3	0.033	0.082	20.0
^{113}Cd CD metal site	−0.270	−0.286	11.9
^{13}C Arg-75 ζ-carbon	0.318	0.351	23.2

[a] δ_P is the paramagnetic contribution to the observed shift. [b] *r* is the distance in angstroms between the nucleus listed plus the EF site.

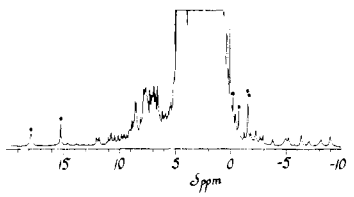

FIGURE 1: ^{1}H NMR spectrum of the parvalbumin–Yb^{3+} complex showing the observed lanthanide-shifted methyl resonances. The 0.68 mM protein sample was prepared in 15 mM Pipes, 0.15 M KCl, 10 mM DTT, and 0.5 mM DSS in D_2O, pH 6.65, at a total metal to total protein ratio of 0.8. The sample temperature was 303 K.

tribution ($\delta_P = \delta_{obsd} - \delta_{diamagnetic}$) to the shift, given that Lu^{3+} causes very similar shifts as Ca^{2+}. For example, Lu^{3+} causes a 0.0113 ppm shift of the C2 proton of His-26, a 0.0384 ppm shift of the C4 proton of His-26, and a 0.0023 ppm shift of the acetyl CH_3 protons from the Ca^{2+} form of parvalbumin (T. C. Williams and B. D. Sykes, unpublished results). These measurements are summarized in Table I. Similarly, six shifted resonances with areas corresponding to three protons can be found outside of the main ^{1}H NMR envelope. All other nonoverlapping shifted resonances have an area equal to one proton [resonances overlapping at any one temperature can in most cases be resolved at a different temperature (Lee & Sykes, 1980b,d)]. These six resonances, seen at 17.79, 15.17, −0.27, −0.80, −1.59, and −1.63 ppm in Figure 1, can therefore be attributed to shifted methyl protons. The diamagnetic positions of these resonances can be estimated by extrapolating their chemical shift as a function of $1/T^2$ to zero (Lee & Sykes, 1980b,d). This procedure yields diamagnetic chemical-shift positions of 0.10, 1.00, 1.35, −0.43, 0.31, and −0.19 ppm, respectively (Lee & Sykes, 1980b). The corresponding paramagnetic shifts are listed in Table II.

Observation of the ^{113}Cd NMR Resonance of ^{113}Cd Bound to the CD Site. Figure 2a shows the ^{113}Cd NMR spectrum of cadmium-substituted parvalbumin at a total Cd^{2+} to total pravalbumin ratio of 2. The two distinct signals of equal intensity observed at −93.34 and −99.55 ppm have been previously attributed to Cd^{2+} ions bound to the EF and CD sites of parvalbumin, respectively (Drakenberg et al., 1978). The previous assignment of the more low-field signal to the EF cadmium has, however, been changed (Vogel et al., 1983), and we will assume herein that the reverse assignment is correct [see Discussion, Lee & Sykes (1981), and Corson et al. (1983)].

When Yb^{3+} is added to the Cd^{2+}-saturated protein at a total Yb^{3+} to total protein ratio of 0.33 (Figure 2b), a decrease in the intensity of the resonance at −99.55 ppm is observed with a concurrent appearance of a new resonance at +2.90 ppm (not shown) corresponding to free Cd^{2+} ions. Further additions of Yb^{3+} result in corresponding decreases in the intensity of the resonance at −99.55 ppm (Figure 2b–e) and increases in the intensity of the resonance at +2.90 ppm (not shown). As

Table II: Comparison of the Observed and Calculated Paramagnetic Shifts and Distances for the 20 Methyl Groups within 15 Å of the EF Site

obsd δ_P	obsd r (Å)[a]	calcd δ_P	calcd nucleus	calcd r (Å)[b]
17.69	6.2 + (0.2/−0.2)	17.76	Leu-86 δ-1	6.14
14.17	7.9 + (1.8/−0.7)	10.17	Ile-97 δ-1	7.19
		6.13	Leu-86 δ-2	8.35
		5.82	Ile-97 γ-2	5.98
		4.39	Leu-63 δ-1	10.13
		3.50	Ile-58 γ-2	9.59
		2.87	Leu-63 δ-2	11.26
		1.87	Thr-82 γ-2	13.20
		1.30	Leu-105 δ-2	10.28
		0.94	Ile-50 γ-2	13.34
		0.60	Ile-58 δ-1	10.24
		0.58	Ile-50 δ-1	14.22
		0.28	Ala-88 β	11.73
		0.18	Leu-105 δ-1	11.18
		+0.17	Val-106 γ-2	13.45
		−0.50	Val-43 γ-1	14.53
−0.37		−0.65	Thr-103 γ-2	14.14
−1.44		−1.22	Ala-104 β	10.68
−1.62		−2.31	Val-99 γ-1	10.76
−1.90		−2.97	Val-99 γ-2	9.02

[a] Calculated from the line widths (Lee & Sykes, 1980c). [b] Calculated from the X-ray crystallographic coordinates.

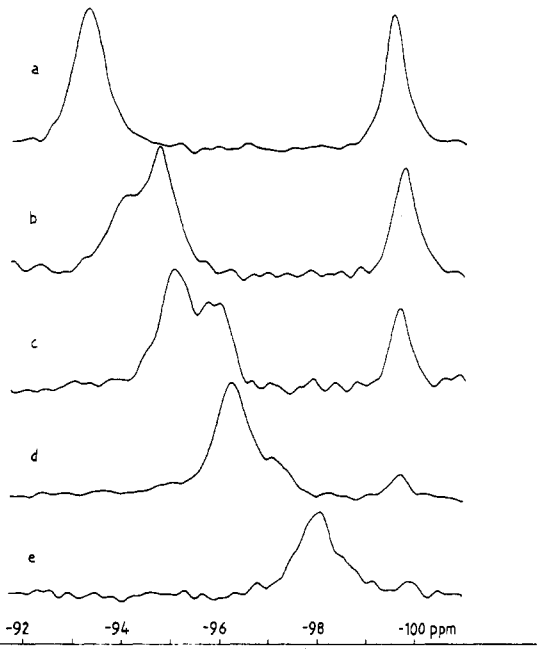

FIGURE 2: ^{113}Cd NMR spectra of 1.27 mM cadmium-saturated carp parvalbumin in 50 mM cacodylate buffer, pH 6.4, at various molar ratios of total ytterbium to total protein: (a) 0, (b) 0.33, (c) 0.67, (d) 1.00, and (e) 1.67.

the ^{113}Cd NMR signal at −99.55 ppm disappears, the signal initially at −93.34 ppm shifts upfield and splits into two resonances. The realtive intensities of these two resonances (Figure 2b–d) indicate that the more downfield of the pair corresponds to $^{113}Cd^{2+}$ in the CD site with Yb^{3+} in the EF site, and the more upfield of the pair corresponds to $^{113}Cd^{2+}$ in the CD site with $^{113}Cd^{2+}$ in the EF site. The chemical shifts for the pairs of CD ^{113}Cd resonances observed in spectra b, c, and d of Figure 2 are (−94.07, −94.72), (−95.16, −95.96), and (−96.28, −97.14) ppm, respectively. The net shift difference for the $^{113}Cd^{2+}$ in the CD site between Yb^{3+} and $^{113}Cd^{2+}$ in the EF site is 0.80 ppm [taken from the spectrum where they are present in almost equal quantities (Figure 2c)]. The upfield shift of both of the pair of CD site ^{113}Cd resonances is

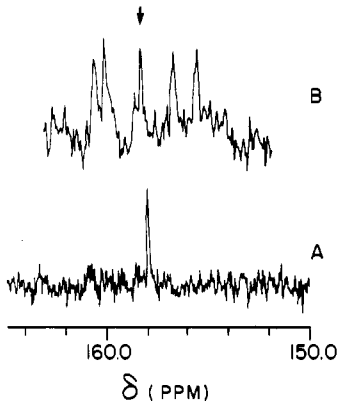

FIGURE 3: ^{13}C NMR spectra of 6.9 mM carp parvalbumin in 0.15 M KCl and 5 mM Pipes, pH 6.5, (A) with no Yb^{3+} or (B) in the presence of 7.2 mM Yb^{3+}.

attributed to the binding of the Cd^{2+} ions released from the EF site by Yb^{3+} to a weak third site near the CD site (Rhee et al., 1981; Vogel et al., 1983). The exchange rate for this process is in the NMR fast exchange limit.

When the diamagnetic lanthanide ion Lu^{3+} ($4f^{14}$ and closest in ionic radius to Yb^{3+}) is added to $^{113}Cd^{2+}$-saturated protein, very similar ^{113}Cd NMR spectra are observed (data not shown). As the ^{113}Cd corresponding to the EF site is displaced, the Cd^{2+} corresponding to the CD site shifts upfield and splits into a pair of resonances, one corresponding to $^{113}Cd^{2+}$ in the CD site with Lu^{3+} in the EF site and one corresponding to $^{113}Cd^{2+}$ in the CD site with $^{113}Cd^{2+}$ in the EF site. In this case, the resonance corresponding to Lu^{3+} occupancy of the EF site is 1.07 ppm more downfield than the resonance corresponding to Cd^{2+} in the EF site. Hence, the net difference in chemical shift of the $^{113}Cd^{2+}$ resonance corresponding to the Cd^{2+} in the CD site resulting from the *paramagnetism* of the lanthanide Yb^{3+} in the EF site is −0.27 ppm (Table I).

Observation of the ^{13}C NMR Resonance of the ζ-Carbon of Arginine-75. The one clearly assignable resonance in the ^{13}C NMR spectrum of carp parvalbumin (Figure 3A) is the signal at 157.900 ppm which corresponds to the ζ-carbon of the single Arg-75 (Nelson et al., 1979). This spectrum was taken in the absence of ^1H decoupling to avoid heating the sample since the lanthanide-induced shifts are very temperature dependent (Lee & Sykes, 1980d). In the presence of 1.1 equiv of Yb^{3+}, several new ^{13}C resonances appear in this region of the spectrum (Figure 3B). The nearest resonance (δ = 158.218) has the most similar intensity and line width to the original ζ-carbon resonance, and it is therefore *attributed* to the shifted ζ-carbon. This gives a paramagnetic shift of 0.318 ppm (Table I). Since this resonance has not ben unequivocally assigned, it has not been used in any fitting procedures but is presented in the comparison of results of the fitting procedures (see Discussion).

Discussion

Determination of the Magnetic Susceptibility Tensor. We have outlined elsewhere the strategy for the analysis of the lanthanide-induced ^1H NMR chemical shifts of the Yb^{3+}–parvalbumin complex in order to determine the three-dimensional structure of the EF binding site of carp parvalbumin in solution (Lee & Sykes, 1980a,b). The substitution of calcium by ytterbium at a total Yb^{3+} to total protein ratio of less than 1 results in a series of shifted resonances corresponding to the filling of a single site on the protein by Yb^{3+} (Lee & Sykes, 1980b, 1981). By analogy to X-ray crystallographic (Sowadski et al., 1978), fluorescence (Horrocks & Sudnick, 1979), and optical (Donato & Martin, 1974) studies, we have concluded that the substitution occurs initially in the EF site (Lee & Sykes, 1981). Thus, these shifted resonances correspond to nuclei in the vicinity of the first site filled, the EF site. [At higher ratios, a new series of resonances appear which correspond to nuclei in the vicinity of the second site filled, the CD site (Lee & Sykes, 1981).]

Three ^1H NMR resonances of carp parvalbumin have been assigned, and their paramagnetic shifts, caused by Yb^{3+} binding to the EF site, have been measured (Lee & Sykes, 1982). The C2 and C4 protons of His-26 have observed paramagnetic shifts of 0.485 and 0.343 ppm, respectively (Table I). Similarly, a paramagnetic shift of 0.033 ppm has been observed for the *N*-acetyl methyl resonance (Table I).

We have presented data herein for the newly assigned ^{113}Cd resonance. Previous ^{113}Cd NMR studies (Drakenberg et al., 1978) indicate the nonequivalence of the CD and EF sites of carp parvalbumin. Two distinct signals of equal intensity (Figure 2) at −93.34 and −99.55 ppm are observed in Cd^{2+}-saturated parvalbumin; they have been attributed to Cd^{2+} ions bound to the EF and CD sites, respectively (Drakenberg et al., 1978). When Yb^{3+} was introduced to the protein at a Yb^{3+} to a protein ratio of 0.67 (Figure 2c), the resonance at −99.55 ppm decreased, and a new resonance corresponding to free Cd^{2+} ions in solution appeared at 2.90 ppm; thus, Yb^{3+} displaces the Cd^{2+} ions in one site, resulting in the release of free Cd^{2+} cations in solution. Since Cd^{2+} displaces Ca^{2+} from the CD and EF sites equally (Vogel et al., 1983), we can assume that Yb^{3+} displaces the Cd^{2+} ions corresponding to the EF site at −99.55 ppm. The previous attribution of the more upfield $^{113}Cd^{2+}$ resonance to the CD site (Drakenberg et al., 1978) has been changed (Vogel et al., 1983). Lanthanide-induced shifts are thus observed for the nearby ^{113}Cd bound in the CD site, 11.9 Å from the EF site (Kretsinger & Nockolds, 1973). In the presence of the paramagnetic Yb^{3+} in the EF site (Figure 2b–d), a shift of 0.80 ppm is observed in the $^{113}Cd^{2+}$ NMR resonance corresponding to Cd^{2+} bound in the CD site. For determination of the diamagnetic shift, the ^{113}Cd NMR spectrum of Cd^{2+}-saturated parvalbumin was determined in the presence of the diamagnetic lanthanide Lu^{3+}. The NMR spectrum indicates a diamagnetic shift of +1.07 ppm for Cd^{2+} bound to the CD site when Lu^{3+} is present in the EF site. These data indicate a paramagnetic shift of −0.27 ppm for the $^{113}Cd^{2+}$ NMR resonance of Cd^{2+} bound to the CD site of parvalbumin. An interesting feature of the lanthanide-induced shifts is that the CD site $^{113}Cd^{2+}$ NMR resonances shift upfield (~3 ppm) as the ratio of Yb^{3+}/parvalbumin increases. The reason for such behavior is unclear; however, it may be due to the influence of metal binding to a proposed third site near the CD site (Rhee et al., 1981).

We have also measured a paramagnetic shift of 0.318 ppm for the ζ-carbon of Arg-75, although the attribution of the shifted resonance must be considered tentative.

Using these assigned resonances, we can determine the orientation and principal elements of the magnetic susceptibility tensor of the Yb^{3+} ion, so that we can relate the paramagnetic shifts to protein structure (eq 1). The five unknowns $L1$, $L2$, α, $A1$, and $A2$ (see Theory of the Lanthanide-Induced Shifts) must be determined. Because we have only four solidly assigned resonances (His-26 C2, His-26 C4, acetyl CH_3, and CD ^{113}Cd) with known position in the X-ray structure, we have included the methyl resonances in our analysis. (There are a total of 20 methyl groups within 15 Å of the EF site.) Two of these methyl resonances are shifted more downfield than 10 ppm, and another four observed methyl resonances are

shifted upfield. The other methyl resonances have not been shifted outside of the main ^1H NMR envelope.

Proton coordinates of nuclei surrounding the metal binding site which are needed to calculate spectra from the crystallographic structure were generated from the last diamond-refined X-ray structure of parvalbumin (Moews & Kretsinger, 1975) by assuming standard bond lengths and geometries. Average methyl proton positions were determined with the "methyl proton centroid" model (Rowan et al., 1974).

The search for the best-fit solution to the NMR unknowns was made in the following manner. For a given choice of $L1$, $L2$, and α, the geometric factors $G1$ and $G2$ (eq 1) were calculated for the His-26 C2 proton, the His-26 C4 proton, the *N*-acetyl CH_3 protons, and the CD ^{113}Cd. The parameters $A1$ and $A2$ for this particular choice of axis system were taken as those giving the best least-squares fit (given the value χ-1) of the calculated shifts to the observed paramagnetic shifts for these four resonances. If the resultant calculated shifts for the four assigned resonances were in reasonable agreement with the observed shifts, the shifts of the methyl groups near the EF site were then calculated from their geometry in this axis system and the best-fit $A1$ and $A2$. This choice of axis system was then rejected if it did not meet the criteria of having only two methyl groups shifted more downfield than 10 ppm and having no methyl resonance shifted more upfield than −5 ppm. If the particular choice of $L1$, $L2$, and α passed the above criteria, the goodness of the fit between the calculated and observed spectra was tested by calculating a χ value (χ-2) which compares the two calculated most downfield methyl shifts with the observed values of $\delta_P = 17.69$ and 15.17 and the calculated most upfield methyl shift with the observed $\delta_P = -1.90$. The best-fit solution was identified on the basis of the minimum χ-1 and χ-2 corresponding to the best fit of the calculated shifts to the His-26 C2, His-26 C4, and *N*-acetyl methyl protons and the ^{113}Cd nucleus and to the three shifted methyl groups. The solution used had $L1 = 0.460$, $L2 = 0.360$, $L3 = 0.812$, $\alpha = 5.25$ rad, $A1 = -1538$ ppm Å^3, and $A2 = 3021$ ppm Å^3. In fact, 24 solutions were found corresponding to the various possible permutations of the labeling of the principal axis system (Agresti et al., 1977). The solution selected, adopting the convention that $|A1|$ be maximal and that $0 < |A2/A1| < 1$, was $L1 = 0.780$, $L2 = 0.500$, $L3 = 0.376$, and $\alpha = 1.17$ rad with the values of $A1$ and $A2$ equal to 2518 and 1113 ppm Å^3, respectively.

Comparison of Observed and Calculated Spectra. The calculated shifts of the four assigned resonances from the best-fit solution obtained in the manner described above are listed in Table I. There is good agreement here between the calculated and observed results, indicated by a standard (χ-1) deviation of +/−0.03 ppm. The paramagnetic shifts for the observed methyl groups and the distances obtained from their line widths (Lee & Sykes, 1980c) are listed in Table II. Also listed are the best-fit calculated shifts and the distances, based upon the X-ray structure. There is fair agreement for the two most downfield-shifted methyl groups (17.69 vs. 17.76 ppm and 14.17 vs. 10.17 ppm). In addition, the calculated distances based upon the X-ray structure (6.14 and 7.19 Å) correspond well with the observed distances [6.2 ± 0.2 and 7.9 + (1.8/−0.7) Å] which were calculated from the line widths of these resonances (Lee & Sykes, 1980c). There is also good agreement for the remaining methyls. Most of the methyl groups are shifted to regions of the spectrum where their resonances are not resolved.

A list of the most downfield observed and calculated shifts is presented in Table III. The six most downfield observed shifts are in the range of 18.90–27.62 ppm. Four resonances with shifts greater than 27.62 ppm are predicted. Also indicated in Table III are the predicted line widths of the shifted resonances relative to the line width of the peak observed at 29.80 ppm (Figure 1). This calculation is based upon a r^6 dependence of the line width (Lee & Sykes, 1980c) and a calculated distance from the observed line width of 5.9 Å for the peak at 29.80 ppm. The α-CH proton of Ile-97 would be too broad to be observable.

Table III: Comparison of the Most Downfield Observed and Calculated Chemical Shifts for CH Protons

	calcd		
obsd δ_P	δ_P	CH nucleus	rel broadening[a]
	39.5	Ile-97 α	25.4
27.62	36.8	Asp-92 β-2	4.8
25.77	36.7	Ile-97 γ-1	3.6
22.26	28.3	Asp-92 β-1	3.8
22.09	25.3	Ile-97 γ-2	1.3
20.10	21.6	Asp-90 β-1	3.5
18.90	17.5	Lys-96 α	2.1

[a] This column indicates the predicted line broadening relative to the line width of the resonance with an observed chemical shift of 29.80 and $r = 5.85$ Å [which was calculated from its line width (Lee & Sykes, 1980c)]. The predicted line broadening is based on a r^6 dependence.

The specific comparisons of the calculated and observed paramagnetic shifts discussed above and listed in Tables I–III indicate that the agreement is very good for the assigned resonances but that deviations as large as 4 ppm are found for some of the methyl groups (i.e., the δ-1 CH_3 of Ile-97) and deviations as large as ~10 ppm are seen for the protons closest to the metal (i.e., the β-2 CH_2 proton of Asp-92). To visualize what these discrepancies mean in terms of distances, we have plotted paramagnetic chemical shift contour surfaces and the protein map in the stereodiagrams (Figures 4–6). Figure 4 shows the 27 ppm chemical shift contour surface; protons within this contour surface (~5–6 Å from the metal ion) have calculated shifts greater than 27 ppm; protons outside this contour surface have calculated shifts less than 27 ppm. Immediately we see that relatively large errors in the calculated paramagnetic shifts can be the result of very small differences in distances.

Figures 5 and 6 show specific examples. In Figure 5, the positions of the protons of Ile-97 are shown in relation to the 14 ppm contour surface which is approximately the observed shift of the δ-CH_3 protons of Ile-97 (Table II). These protons lie outside the 14 ppm contour surface by ~0.6 Å. Given the information that the chemical shift of the γ-1 CH proton of Ile-97 is calculated to be too large (Table III), this suggests that shifts of both these protons could be brought into closer agreement by a slight rotation of the orientation of a portion of Ile-97 to bring the δ-CH_3 group approximately 0.6 Å closer to the metal and to move the γ-CH proton correspondingly farther away.

Similarly, Figure 6 shows the orientation of Asp-92 and the 27 ppm chemical shift contour surface which corresponds to the largest observed shift. One of the β-protons has a calculated shift of 28.3 ppm and lies near this contour surface whereas the other has a calculated shift of 36.8 ppm and lies approximately 0.5 Å outside the contour surface. The Asp-92 residue would have to move ≤0.5 Å away from the metal to bring the calculated and observed shifts into closer agreement.

Sources of Error. For protons which are close to the metal ion (5–10 Å), the calculated paramagnetic shifts based upon the X-ray structure are generally larger than the corresponding

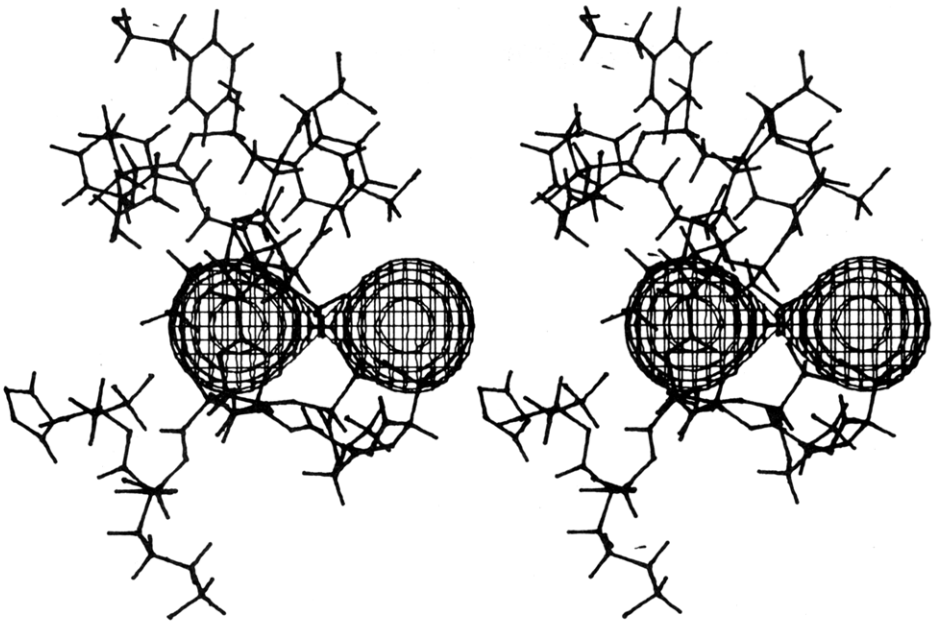

FIGURE 4: Orientation of the 27 ppm chemical shift contour surface for Yb^{3+} bound to the EF site of carp parvalbumin. The protein map contains residues closer than ~15 Å to the EF site metal ion. Protons bound to carbon and nitrogen atoms are included in the protein map. For methyl protons, the methyl centroid model was used in which the C–C bond has been extended linearly by 0.366 Å to give an effective position for the methyl protons. Carbonyl oxygens are not included. The cross hairs indicate the position of the Yb^{3+}. The chemical shift contour surface shown represents those positions in the protein which have a paramagnetic-induced shift of 27 ppm. The contour surface has been plotted with a 0.5-Å grid. The distance between the two lobe extremities is ~11 Å. The protein map and the contour surface are shown in the principal axis system of the magnetic susceptibility tensor of the Yb^{3+} in the EF site. The orientation shown is the XZ plane with the positive z axis horizontal and to the right and the positive y axis into the page. The six ligands to the metal have the following orientations: Asp-90, x; Asp-92, z; Asp-94, $-y$; Lys-96, $-z$; Gly-98, $-x$; Glu-101, y.

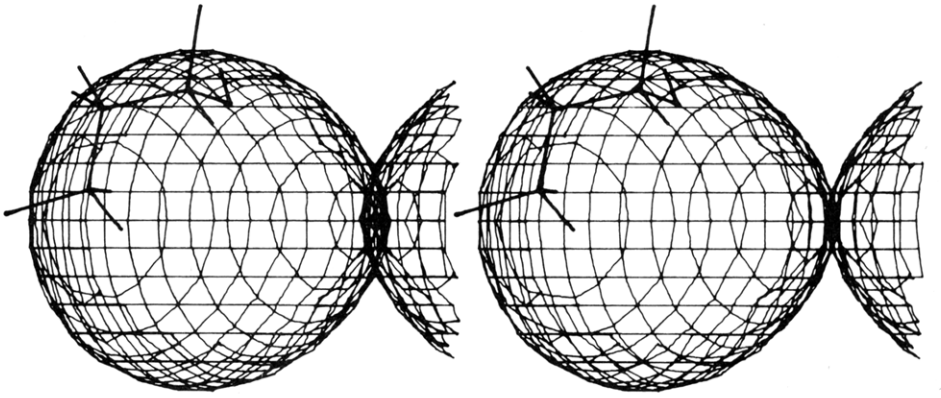

FIGURE 5: Relative orientation of isoleucine-97 and the 14 ppm paramagnetic chemical shift contour surface. In this diagram, the principal axis system of the Yb^{3+} magnetic susceptibility tensor and the protein has been rotated 35° around the x axis relative to the orientation in Figure 4 so that the $-z$ axis is coming partially out of the page. The α-CH proton and the two γ-CH_2 protons can be seen inside the 14 ppm chemical shift contour surface, whereas the β-CH proton and the β- and δ-CH_3 protons are outside this surface. The chemical shift contour surface is drawn with a 0.5-Å grid.

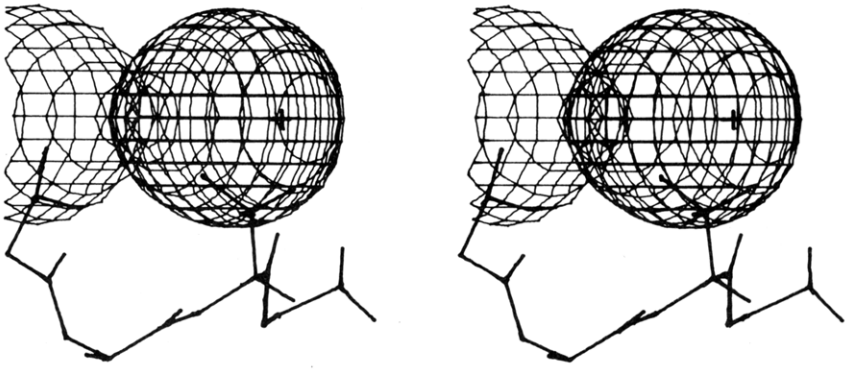

FIGURE 6: Relative orientation of Asp-92, Gly-93, Asp-94, and the 27 ppm paramagnetic chemical shift contour surface. In this diagram, the principal axis system and the protein have been rotated −44° around the x axis relative to the orientation shown in Figure 4 so that the z axis is pointing partially out of the page. Both β-CH_2 protons of Asp-92 and the carboxyl carbon can be seen inside this contour surface, with one β-CH_2 proton just touching this surface. The chemical shift contour surface is plotted with a 0.5-Å grid.

observed shifts (see Tables II and III). This implies that the NMR is "indicating" a more open structure that is less compact than the X-ray structure near the metal binding site. There are several potential problems in the analysis, from both the NMR and the X-ray standpoints which are discussed below.

In the NMR analysis, the position of Yb^{3+} was assumed to be identical with that position observed for Ca^{2+} in the crystallographic structure. Slight differences in position would result in systemic changes in atom positions of all residues, but this would result in some atoms being closer to the metal and some being farther away. Similarly, the neglect of scalar interactions may not be accurate for some nuclei; however, the sign of the effect would again vary.

More significant possible problems from the NMR point of view are the possibility that the principal axis system is not yet perfect, that the Yb^{3+} structure is different from the Ca^{2+} structure, and that motional averaging influences the NMR results. From the standpoint of the determination of the principal axis system of the Yb^{3+} magnetic susceptibility tensor, the assigned residues we used were far removed from the metal and at relatively diverse angular orientations so that small errors in geometry are not expected to have a large effect. Also, the orientation determined was not greatly sensitive to the exact values of the shifts used for the assigned residues. However, this diagonalization procedure was certainly not experimentally overdetermined.

From the standpoint of differences between the Yb^{3+} and Ca^{2+} structures, the changes would have to be in the direction of a more open Yb^{3+} structure. This is not likely given the similar ionic radius of Yb^{3+} and Ca^{2+} and the tighter binding of Yb^{3+} to the protein. The X-ray studies of Matthews & Weaver (1974) on thermolysin with a series of lanthanide metal ions indicated structural changes on the order of a few tenths of an angstrom. The structural changes were the smallest, however, for the lanthanides of higher atomic number such as Yb^{3+}, presumably because of the closer similarity of their ionic radii to that of calcium. In the X-ray structure of parvalbumin, Tb^{3+} was used in place of Ca^{2+} as an isomorphous heavy-atom derivative (Sowadski et al., 1978).

Certainly, the NMR structure is a motionally averaged structure, and this may account for the differences observed. However, the form of the dependence of the shifts on distance ($\alpha\ 1/r^3$) is such that averaging over any harmonic potential would lead to observed shifts larger than expected because of shorter average effective distances. If a large amount of motion were present with the protons spending a large fraction of time farther from the metal, averaging could give effective larger distances and smaller observed shifts.

Other potential contributions reside at the level of the X-ray crystallographic analysis of the Ca^{2+}-saturated parvalbumin. The parvalbumin structure was determined from nominal 1.9-Å resolution data, but bad contacts and disorted ring geometries are observed. In particular, a motional disorder of the amino-terminal residues was observed (Moews & Kretsinger, 1975) which includes the acetyl CH_3 protons used in the NMR analysis. The refinement of the parvalbumin structure, which has not been reported to date, may point to changes which are not large but significant as far as the NMR analysis is concerned. Moreover, other sources of error may result from the calculations which were performed on the crystallographic coordinates. In particular, inaccuracies in proton coordinates may result from the method of proton coordinate generation which was based upon standard bond geometries and bond lengths. Finally, there may be errors due to the method of methyl proton coordinate generation based upon the methyl centroid model (Rowan et al., 1974).

Acknowledgments

We thank Drs. S. Forsén and T. Drakenberg of the Chemical Centre, Lund, Sweden, for obtaining the ^{113}Cd NMR spectra and Dr. I. D. Kuntz (University of California, San Francisco) for helpful discussions. The assistance of Dr. Tom Nakashima and Glen Bigam in obtaining the ^{13}C NMR spectra is also acknowledged. We thank Gerard McQuaid for his meticulous upkeep of the NMR spectrometer and Michael Nattriss for running the amino acid analyses. We acknowledge Colin Broughton and Masao Fujinaga for their help in preparing the stereodiagrams.

Registry No. Ytterbium, 7440-64-4; lutecium, 7439-94-3.

References

Agresti, D. G., Lenkinski, R. E., & Glickson, J. C. (1977) *Biochem. Biophys. Res. Commun. 76*, 711.

Birnbaum, E. R., & Sykes, B. D. (1978) *Biochemistry 17*, 4865.

Bleaney, B. (1972) *J. Magn. Reson. 8*, 91.

Briggs, J. M., Moss, G. P., Randall, E. W., & Sales, K. D. (1972) *J. Chem. Soc., Chem. Commun.*, 1180.

Collins, J. H. (1974) *Biochem. Biophys. Res. Commun. 58*, 301.

Collins, J. H. (1976) *Nature (London) 259*, 699.

Collins, J. H., Greaser, M. L., Potter, J. D., & Horn, M. J. (1977) *J. Biol. Chem. 252*, 6356.

Corson, D. C., Lee, L., McQuaid, G. A., & Sykes, B. D. (1983) *Can. J. Biochem.* (in press).

Dedman, J. R., Jackson, R. L., Schreiber, W. E., & Means, A. R. (1978) *J. Biol. Chem. 253*, 343.

Donato, H., Jr., & Martin, R. B. (1974) *Biochemistry 13*, 4575.

Drakenberg, T., Lindman, B., Cave, A., & Parello, J. (1978) *FEBS Lett. 92*, 346.

Fullmer, C. S., & Wasserman, R. H. (1977) in *Calcium Binding Proteins and Calcium Function* (Wasserman, R. H., Corradino, R. A., Carafoli, E., Kretsinger, R. H., MacLennan, D. H., & Siegel, F. L., Eds.) p 302, Elsevier, New York.

Hofmann, T., Kawakami, M., Hitchman, A. J. W., Harrison, J. E., & Dorrington, K. J. (1979) *Can. J. Biochem. 57*, 737.

Horrocks, W. DeW., Jr., & Sudnick, D. R. (1979) *J. Am. Chem. Soc. 101*, 334.

Kretsinger, R. H. (1976) *Annu. Rev. Biochem. 45*, 239.

Kretsinger, R. H., & Nockolds, C. E. (1973) *J. Biol. Chem. 248*, 3313.

Lee, L., & Sykes, B. D. (1980a) *Adv. Inorg. Biochem. 2*, 183.

Lee, L., & Sykes, B. D. (1980b) *Biophys. J. 32*, 193.

Lee, L., & Sykes, B. D. (1980c) *Biochemistry 19*, 3208.

Lee, L., & Sykes, B. D. (1980d) *J. Magn. Reson. 41*, 512.

Lee, L., & Sykes, B. D. (1981) *Biochemistry 20*, 1156.

Lee, L., & Sykes, B. D. (1982) *Biomolecular Structure Determination by NMR* (Bothner-By, A. A., Glickson, J. D., & Sykes, B. D., Eds.) pp 169–188, Marcel Dekker, New York.

Marinetti, T. D., Snyder, G. H., & Sykes, B. D. (1977) *Biochemistry 16*, 647.

Matthews, B. W., & Weaver, L. H. (1974) *Biochemistry 13*, 1719.

Moews, P. C., & Kretsinger, R. H. (1975) *J. Mol. Biol. 91*, 201.

Nelson, D. J., Theoharides, A. J., Nieburgs, A. C., Murray, R. K., Gonzalez-Fernandez, F., & Brenner, D. (1979) *Int. J. Quantum Chem. 16*, 159.
Pechere, J.-F., Demaille, J., & Capony, J.-P. (1971) *Biochim. Biophys. Acta 236*, 391.
Reuben, J. (1973) *J. Magn. Reson. 11*, 103.
Rhee, M. J., Sudnick, D. R., Arkle, V. K., & Horrocks, W. DeW., Jr. (1981) *Biochemistry 20*, 3328.
Rowan, R., III, McGammon, J. A., & Sykes, B. D. (1974) *J. Am. Chem. Soc. 96*, 4773.
Sowadski, J., Cornick, G., & Kretsinger, R. H. (1978) *J. Mol. Biol. 124*, 123.
Stevens, F. C., Walsh, M., Ho, H. C., Teo, T. S., & Wang, J. H. (1976) *J. Biol. Chem. 251*, 4495–4500.
Vanaman, T. C., Sharief, F., & Watterson, D. M. (1977) in *Calcium Binding Proteins and Calcium Function* (Wasserman, R. H., Corradino, R. A., Carafoli, E., Kretsinger, R. H., MacLennan, D. H., & Siegel, F. L., Eds.) p 107, Elsevier, New York.
Vogel, H. J., Drakenberg, T., & Forsén, S. (1983) in *NMR of Newly Accessible Nuclei* (Laslo, P., Ed.) Academic Press, New York.
Weeds, A. G., & McLachlan, A. D. (1974) *Nature (London) 252*, 646.

Resonance Raman Studies of Carbon Monoxide Binding to Iron "Picket Fence" Porphyrin with Unhindered and Hindered Axial Bases. An Inverse Relationship between Binding Affinity and the Strength of Iron–Carbon Bond†

Ellen A. Kerr, Helen C. Mackin, and Nai-Teng Yu*

ABSTRACT: The stretching frequency of the iron–carbon bond, ν(Fe–CO), is a direct measure of the iron–carbon bond strength when there is no change in the Fe–C–O geometry. Here we report resonance Raman detection of ν(Fe–CO) frequencies in the CO complexes of iron(II) $\alpha,\alpha,\alpha,\alpha$-*meso*-tetrakis(*o*-pivalamidophenyl)porphyrin, Fe^{II}(TpivPP), with trans ligands of varying strength: *N*-methylimidazole (*N*-MeIm), 1,2-dimethylimidazole (1,2-Me_2Im), pyridine (py), and tetrahydrofuran (THF). It was found that the weaker the iron–trans ligand bond, the stronger the iron–carbon bond. Comparisons of sterically hindered (1,2-Me_2Im) and unhindered (*N*-MeIm) bases are of particular interest because of their implication in the phenomenon of hemoglobin cooperativity and the mechanisms of protein control of heme reactivity. While the CO binding affinity of Fe^{II}(TpivPP)(1,2-MeIm) is ~400 times lower than that of Fe^{II}(TpivPP)(*N*-MeIm), the ν(Fe–CO) frequency for the former (at 496 cm^{-1}) is higher than that for the latter (at 489 cm^{-1}). This example shows that the CO binding affinity cannot be directly correlated with the strength of the iron–carbon bond. Comparison of the CO binding to Fe^{II}(TpivPP)(THF) and Fe^{II}(TpivPP)(*N*-MeIm) reveals a similar relationship; the ν(Fe–CO) frequency (at 527 cm^{-1}) in Fe^{II}(TpivPP)(THF)(CO) is 38 cm^{-1} higher than that in Fe^{II}(TpivPP)(*N*-MeIm)(CO), but the CO binding affinity is lower for the THF complex. This implies that the free energy change associated with CO binding is not localized at the Fe–C bond; there must be a charge redistribution upon ligand binding so that some free energy compensation has occurred among many chemical bonds.

Carbon monoxide is an excellent Raman–visible ligand for probing the nature of active sites in hemoproteins (Tsubaki et al., 1982). It binds to practically any ferro heme reversibly, and its geometry is subject to distal steric effect (Huber et al., 1970; Norvell et al., 1975; Padlan & Love, 1975; Heidner et al., 1976; Steigemann & Weber, 1979; Baldwin, 1980). Tsubaki et al. (1982) first identified the Fe–CO stretching, Fe–C–O bending, and C–O stretching vibrations in the resonance Raman spectra of carbonmonoxy human hemoglobin A and carbonmonoxy sperm whale myoglobin. The Fe–CO stretching vibration, readily detectable upon Soret excitation, is of particular interest and importance because of its anticipated sensitivity to geometry and to both σ and π back-bonding. The bound C–O stretching vibration has been extensively studied by infrared spectroscopy (Alben & Caughey, 1968; Caughey et al., 1969; Caughey, 1970; Caughey et al., 1973; Barlow et al., 1976; Yoshikawa et al., 1977; Makinen et al., 1979; O'Keefe et al., 1978; Caughey et al., 1978; Caughey, 1980; Alben et al., 1981). However, it may respond more to changes in the π back-bonding than to the electron density in the Fe–CO σ bond.

In recent years considerable research has been directed toward elucidating the detailed structure of the heme, its immediate environment in various hemoproteins, and ligand binding affinities. Much effort has now been focused on the synthesis and study of heme models capable of coordinating molecular oxygen reversibly without autoxidation of Fe^{II} to Fe^{III}. The so-called "picket fence" porphyrins (Collman et al., 1975) with hydrophobic pickets are capable of binding dioxygen and carbon monoxide reversibly at room temperature and thus may be considered as an excellent model system for hemoglobin and myoglobin.

Resonance Raman studies of dioxygen binding to picket fence porphyrins have been reported (Burke et al., 1978; Walters et al., 1980; Hori & Kitagawa, 1980). In this paper, we study the binding of CO to picket fence porphyrins to examine the influence of a trans ligand upon the strength of the Fe–C bond. The effect of distal steric hindrance on the Fe–C bond in carbonmonoxy "strapped hemes" has been reported elsewhere (Yu et al., 1983).

In the absence of steric hindrance as in the case of picket fence porphyrins, the Fe–C–O linkage is presumably linear

† From the School of Chemistry, Georgia Institute of Technology, Atlanta, Georgia 30332. *Received March 16, 1983.* This work was supported by National Institutes of Health Grant GM 18894. Presented in part at the 26th Annual Meeting of the Biophysical Society, Feb 1982 (Kerr et al., 1982).

0006-2960/83/0422-4373$01.50/0